Available online at www.sciencedirect.com

SCIENCE DIRECT®

Bioorganic & Medicinal Chemistry Letters 15 (2005) 2097–2102

Bioorganic & Medicinal Chemistry Letters

QSAR analyses of conformationally restricted 1,5-diaryl pyrazoles as selective COX-2 inhibitors: application of connection table representation of ligands

S. Prasanna,* E. Manivannan and S. C. Chaturvedi

School of Pharmacy, Devi Ahilya Vishwavidyalaya, Ring Road, Indore-452017, India

Received 24 December 2004; revised 10 February 2005; accepted 12 February 2005
Available online 19 March 2005

Abstract—As a part of our continuing efforts in discerning the structural and physicochemical requirements for selective COX-2 over COX-1 inhibition among the fused pyrazole ring systems, herein we report the QSAR analyses of the title compounds. The conformational flexibility of the title compounds was examined using a simple connection table representation. The conformational investigation was aided by calculating a connection table parameter called fraction of rotable bonds, b_rotR encompassing the number of rotable bonds and b_count, the number of bonds including implicit hydrogens of each ligand. The hydrophobic and steric correlation of the title compounds towards selective COX-2 inhibition was reported previously in one of our recent publications. In this communication, we attempt to calculate Wang–Ford charges of the non-hydrogen common atoms of AM1 optimized geometries of the title compounds. Owing to the partial conformational flexibility of title compounds, conformationally restricted and unrestricted descriptors were calculated from MOE. Correlation analysis of these 2D, 3D and Wang–Ford charges was accomplished by linear regression analysis. 2D molecular descriptor b_single, 3D molecular descriptors glob, std_dim3 showed significant contribution towards COX-2 inhibitory activity. Balaban *J*, a connectivity topological index showed a negative and positive contribution towards COX-1 and selective COX-2 over COX-1 inhibition, respectively. Wang–Ford charges calculated on C^7 showed a significant contribution towards COX-1 inhibitory activity whereas charges calculated on C^8 were crucial in governing the selectivity of COX-2 over COX-1 inhibition among these congeners.

Non-steroidal anti-inflammatory drugs (NSAIDs) are widely used for the treatment of pain and inflammation especially arthritis, arthritis-associated disorders.[1] The rate limiting step in the synthesis of prostaglandins and thromboxanes is the conversion of arachidonate to prostaglandin H_2, which is catalyzed by cyclooxygenase (COX) enzymes. Following the discovery of the inducible isozyme cyclooxgenase-2 in 1991 and with the advent of several selective COX-2 inhibitors, still selective inhibition of COX-2 over COX-1 continued to be an attractive target for anti-inflammatory therapy. The major breakthrough in this area came with the initial findings that DuP-697,[2] a diaryl heterocycle (Fig. 1) was anti-inflammatory but not ulcerogenic. Some of the selective COX-2 inhibitors with proven therapeutic utility for the treatment of inflammation include Celecoxib,[3] Rofecoxib,[4] Valdecoxib[5] and Etoricoxib.[6] The investigations of selective COX-2 inhibitors in the treatment of colon cancer, Parkinson's and Alzheimer's disease are the current highly interesting areas of research in this therapeutic area. Abundant of information regarding the diaryl heterocycles as selective COX-2 inhibitors are found in the literature. However, a search

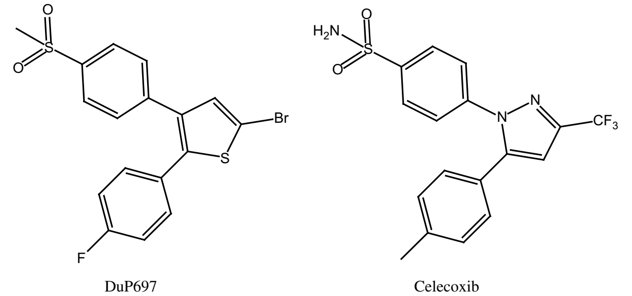

Figure 1. Structures of DuP697 and Celecoxib.

Keywords: QSAR; COX-2; COX-1; MOE and connection table representation.

* Corresponding author at present address: Department of Medicinal Chemistry, School of Pharmacy, 417 Faser Hall, University, Mississippi, 38677, USA; e-mail: prasu05@rediffmail.com

0960-894X/$ - see front matter © 2005 Elsevier Ltd. All rights reserved.
doi:10.1016/j.bmcl.2005.02.035

of literature for fused heterocycles as template revealed only few citations for selective COX-2 inhibition. Hence we focused our attention in considering the fused heterocyclic ring systems as a part of our research efforts.[7–11]

Recently, we reported[12] QSAR analysis of two series of fused pyrazoles as selective COX-2 inhibitors. In this communication, we report the QSAR studies of conformationally restricted 1,5-diaryl pyrazoles in continuation with our previous preliminary findings.[12] The chosen series[13] consists of 15 compounds with a central pyrazole ring fused to the non-sulfonyl benzene ring of common diaryl heterocycles type of selective COX-2 inhibitors. Table 1 lists all the title compounds with their observed activity.

QSAR models were built using the regression analysis module of systat version 10.2. The correlation matrix was used to correlate the biological activity with the various predictor variables. Descriptors with inter correlation above $|r| > 0.5$ are not considered while deriving QSAR models. The predictor variables with p value greater than 0.05 were eliminated whilst deriving the QSAR models in order to assure their statistical reliability. The QSAR models were evaluated by using the statistical parameters viz., correlation coefficient (r) or coefficient of determination (r^2), adjusted r^2 (r^2_{Adj}), standard error of estimate (s), Fischer F-value and student's t-distribution. The latter is used to assess the significance of the individual regression terms. The figures within the parentheses following the coefficient terms are the standard error of the regression terms and the constants. Durbin–Watson (DW) test[14] was employed to check the serial correlation in residuals. Since the DW values in all our derived models are greater than 1.4, there is probably not any serious auto correlation in the residuals. A data point is considered as an outlier if it has a large magnitude (when the residual value exceeds twice the standard error of estimate of the model). Self-consistency of the derived models is ensured using the leave-one-out (Loo) cross-validation process and the predictability of each model was assessed using cross-validated r^2 or q^2.

Recently, the calculation of Wang–Ford charges gained recognition in QSAR studies[15–17] in exploring the binding mode of ligands towards their biological targets. Semi-empirical Austin Model 1 method[18,19] was used to optimize the geometry of the title compounds. For the calculation of Wang–Ford charges, the non-hydrogen common atoms of the minimum energy conformers were given same serial numbers in all the models. Figure 2 shows the title compounds with common atoms numbered for the calculation of Wang–Ford charges. Figure 3 shows the AM1 optimized geometries of most active compounds of the series. Energy minimization (using restricted Hartree–Fock: closed shell wave function) and Wang–Ford charge calculations were accomplished using Chem 3D ultra 6.0.1 software.[20]

The conformational restriction of these compounds is attributed to the fusion of non-sulfonyl benzene ring with central pyrazole ring. In order to examine the partial conformational flexibility of these compounds we attempted to derive structure connectivity representation

Table 1. Conformationally restricted 1,5-diaryl pyrazoles and their observed activities

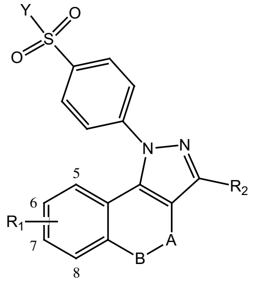

Compd no	A	B	R_1	R_2	Y	Observed activity		
						$pIC_{50(COX\text{-}2)}$ (M)	$pIC_{50(COX\text{-}1)}$ (M)	$\log[IC_{50(COX\text{-}1)}/IC_{50(COX\text{-}2)}]$
1	S	CH_2	H	CF_3	NH_2	7.70	6.40	1.30
2	CH_2	CH_2	H	CF_3	NH_2	5.96	4.87	1.09
3	CH_2	S	H	CF_3	NH_2	6.34	5.01	1.32
4	CH_2	O	H	CF_3	NH_2	5.88	5.15	0.72
5	S	CH_2	$7CH_3$	CF_3	NH_2	7.66	6.10	1.56
6	S	CH_2	$7OCH_3$	CF_3	NH_2	7.89	6.52	1.36
7	S	CH_2	$7OCH_3$, 8F	CF_3	NH_2	8.05	5.56	2.48
8	S	CH_2	7F	CF_3	NH_2	7.40	6.57	0.84
9	S	CH_2	$7CH_3$, 8F	CF_3	NH_2	7.80	4.95	2.84
10	S	CH_2	8F	CF_3	NH_2	7.68	5.20	2.47
11	S	CH_2	7,8diF	CF_3	NH_2	8.22	5.57	2.58
12	S	CH_2	$7OCH_3$, 8F	CF_2H	NH_2	7.49	—	—
13	S	CH_2	$7OCH_3$, 8F	CF_3	CH_3	7.12	—	—
14	S–O	CH_2	$7OCH_3$, 8F	CF_3	NH_2	5.82	—	—
15	S	CH_2	7F	CN	NH_2	6.85	6.12	0.70

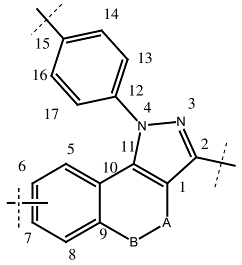

Figure 2. Conformationally restricted 1,5-diaryl pyrazoles with their non-hydrogen common atoms labelled for Wang–Ford charge calculations.

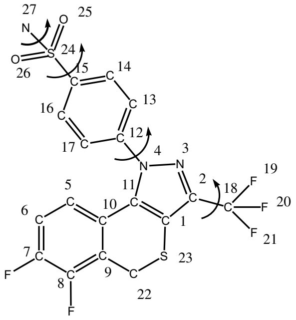

Figure 4. Hydrogen suppressed graph of most active compound 11 of the series showing the partial conformational flexibility.

Table 2. Parameters related to connection table representation of title compounds

Compd No	b_rotN	b_count	b_rotR
1	4	42	0.095238
2	4	44	0.090909
3	4	42	0.095238
4	4	42	0.095238
5	5	45	0.111111
6	6	46	0.130435
7	6	46	0.130435
8	4	42	0.095238
9	5	45	0.111111
10	4	42	0.095238
11	4	42	0.095238
12	6	46	0.130435
13	6	47	0.127660
14	6	49	0.122449
15	4	43	0.093023

of the compounds. b_rotN, which is the number of rotable bonds, was calculated for each ligand. For the present study a bond is considered rotable if it is not in a ring and neither atom of the bond is such that $(d_i + h_i) < 2$, where d is the number of heavy atoms (atoms that have an atomic number strictly greater than 1) to which it is bonded. Hence d is the number of bonded neighbours of the atom in the H suppressed graph. h is the hydrogen count. It is the number of hydrogens to which it is attached. Figure 4 shows the Hydrogen suppressed graph of active member of the series, compound 11. In Figure 4, the hydrogen count, h of N-27 atom is 2 (2 hydrogens are attached to N-27 and is not shown in this Hydrogen suppressed graph) and $d = 1$ (as N-27 is attached to only one S-24 heavy atom). In the same figure for S-24, $d = 4$ and $h = 0$ hence neither atom of the bond N-27–S-24 is $d_i + h_i < 2$ rendering the bond between them as one of the rotable single bonds. Like wise other possible rotable single bonds of compound number 11 include S-24–C-15, C-12–N-4 and C-2–C-18. Fraction of rotable bonds, b_rotR is calculated as b_rotN divided by b_count, the number of bonds including implicit hydrogens. The values of all the parameters used in conformational studies are listed in Table 2. All these studies show that there exists some partial conformational flexibility of these ligands. So we attempted to investigate the correlation of conformationally dependent 3D molecular descriptors towards the COX-2 inhibitory activity. For this purpose some conformationally dependent descriptors were calculated from molecular operating environment (MOE 2002.03), supplied by the Chemical Computing Group Inc. Structures of all compounds were sketched using molecular builder of MOE and each structure was subjected to energy minimization using the MMFF94 force field. Three

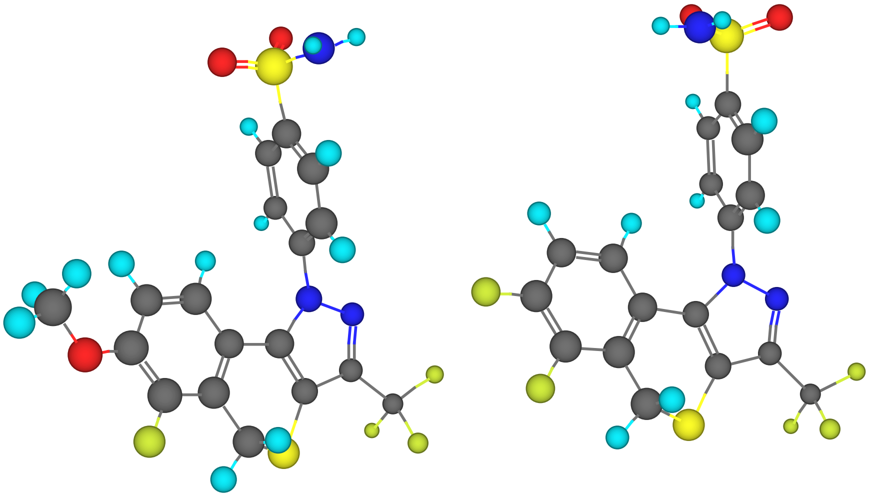

Figure 3. AM1 optimized geometries of most active compounds (compounds 7 and 11).

optimization methods were used in succession namely first steepest descent, then conjugate gradient and finally truncated Newton. QuaSAR-descriptor module of MOE was used to calculate 3D molecular descriptors. 3D molecular descriptors of MOE include, internal 3D (i3D), which use 3D coordinate information about each molecule and external 3D (x3D), which use 3D coordinate information with an absolute frame of reference. A complete list of all the 3D molecular descriptors along with 2D descriptors, which use the atoms and connection information of the molecules, was given in Table 3. All the parameters used in structure representation calculations were derived from MOE.

COX-1 and COX-2 in vitro inhibitory activity are reported[13] as IC_{50} in micromolar units, where IC_{50} is the drug concentration required to inhibit 50% of the enzymes. For the present QSAR study the reported IC_{50} was converted to negative logarithm (pIC_{50}) in molar units. The observed activity was considered as dependent variable and the calculated physicochemical properties as independent variables while modelling statistically significant relationships to explore the selectivity requirements among these compounds. The quantitative model building is limited to triparametric for COX-2 inhibitory activity modelling and biparametric for COX-1 and selective COX-2 over COX-1 inhibitory activity in accordance to general accepted rule of thumb. Some of the statistically sound models are discussed below:

Table 3. Conformationally dependent and independent descriptors used for the present study

2D adjacency and distance matrix descriptors
Balaban *J*
diameter
Petitjean
radius
VDistEq
VDistMa
WeinerPath
WeinerPol
2D atom counts and bond counts
a_aro
a_count
a_heavy
a_nH
a_nC
a_nN
a_nO
a_nS
b_single
b_double
b_triple
b_heavy
VAdjMa
3D surface area, volume and shape descriptors
ASA
dens
glob
pmi
pmiX
pmiY
pmiZ
rgyr
std_dim1
std_dim2
std_dim3
vol
VSA

$$\begin{aligned} pIC_{50(\text{COX-2})} &= -17.143(\pm 2.216)\text{std\_dim3} + 26.818(\pm 2.536)\\ &n = 14,\ r = 0.913,\\ &r^2 = 0.833,\ r^2_{\text{Adj}} = 0.819,\\ &s = 0.360,\ F = 59.86,\\ &p = 0.000,\ q^2 = 0.7464,\\ &\text{DW} = 1.792 \quad \text{outlier}: \text{A} = \text{S},\\ &\text{B} = \text{CH}_2,\ \text{R}_1 = 7\text{F},\ \text{R}_2 = \text{CN},\\ &\text{Y} = \text{NH}_2 \qquad \text{(model 1)} \end{aligned}$$

Model 1 is a monoparametric equation modelled for COX-2 inhibitory activity of 14 compounds. Compound 15 was omitted as outlier while deriving model 1. Compound 15 is the only compound with CN substitution on central pyrazole ring whereas other compounds of the congener possess either triflouro or diflouro methyl groups, the substitution comparable with celecoxib (Fig. 1). The single 3D molecular descriptor, std_dim3 explains 81.9% variance in COX-2 inhibitory activity. std_dim3 is the square root of the third largest eigen value of the covariance matrix of the atomic coordinates of ligand. A standard dimension is equivalent to the standard deviation along a principal component axis.

$$\begin{aligned} pIC_{50(\text{COX-2})} &= -0.164(\pm 0.037)\text{b\_single} - 56.975(\pm 5.812)\text{glob} + 19.550(\pm 1.564)\\ &n = 14,\ r = 0.948,\\ &r^2 = 0.898,\ r^2_{\text{Adj}} = 0.880,\\ &s = 0.294,\ F = 48.55,\\ &p = 0.000,\ q^2 = 0.8399,\\ &\text{DW} = 2.802 \quad \text{outlier}: \text{A} = \text{S},\\ &\text{B} = \text{CH}_2,\ \text{R}_1 = 7\text{F},\ \text{R}_2 = \text{CN},\\ &\text{Y} = \text{NH}_2 \qquad \text{(model 2)} \end{aligned}$$

Model 2 is developed for 14 compounds after eliminating compound 15 as outlier, the reason being the same as explained under model 1. Model 2 explains 88.0% variance in COX-2 inhibitory activity. b_single is a 2D molecular descriptor, basically a type of atom and bond count class of descriptors of MOE. 2D molecular descriptor of MOE is a numerical property that can be calculated from connection table representation of a molecule. b_single refers to number of single bonds of ligands including the implicit hydrogens. Aromatic bonds are not considered to be single bonds during its calculation. A small negative coefficient of b_single shows an unfavourable effect towards COX-2 inhibitory activity. Glob, also designated sometimes as globularity is a 3D molecular descriptor of surface area, volume and shape type descriptors of MOE. Globularity or inverse condition number is basically smallest eigen value divided by the largest eigen value of the covariance matrix of the atomic coordinates of ligand. A value of 1 indicates a perfect sphere while of 0 indicates a two or one dimensional object. It is also related to molecular flexibility. The contribution of glob in model 2 indicates that the COX-2 inhibitory activity depends on the shape and rigidity of the ligands. A list of other 3D molecular descriptors that depend on conformation of ligands is given in Table 3. Both the descriptors used to build model 2 are reasonably orthogonal ($|r| = 0.353$).

$$\begin{aligned}
pIC_{50(\mathrm{COX\text{-}1})} &= 3.829(\pm0.558)C^7 + 5.117(\pm0.111)\\
&n = 10,\ r = 0.925,\\
&r^2 = 0.855,\ r^2_{\mathrm{Adj}} = 0.837,\\
&s = 0.268,\ F = 47.15,\\
&p = 0.000,\ q^2 = 0.7949,\\
&\mathrm{DW} = 2.661 \quad \text{outliers}: \mathrm{A} = \mathrm{S},\\
&\mathrm{B} = \mathrm{CH_2},\ \mathrm{R_1} = \mathrm{H},\ \mathrm{R_2} = \mathrm{CF_3},\\
&\mathrm{Y} = \mathrm{NH_2};\ \mathrm{A} = \mathrm{S},\ \mathrm{B} = \mathrm{CH_2},\\
&\mathrm{R_1} = 7\mathrm{OCH_3},\ 8\mathrm{F},\ \mathrm{R_2} = \mathrm{CF_3},\\
&\mathrm{Y} = \mathrm{NH_2} \qquad \text{(model 3)}
\end{aligned}$$

Model 3 is a monoparametric equation developed for available COX-1 inhibitory activity data. Compounds 1 and 7 are eliminated as outliers while deriving model 3. Model 3 explains 83.7% variance in COX-1 inhibitory activity. The contribution of C^7 in model 3 suggests that COX-1 inhibitory activity could be influenced by substitution at seventh position of the non-sulfonyl benzene ring.

$$\begin{aligned}
pIC_{50(\mathrm{COX\text{-}1})} &= 1.325(\pm0.227)\mathrm{a\_nS}\\
&\quad - 45.911(\pm8.187)\mathrm{Balaban}\ J\\
&\quad + 74.503(\pm12.551)\\
&n = 10,\ r = 0.934,\\
&r^2 = 0.872,\ r^2_{\mathrm{Adj}} = 0.836,\\
&s = 0.267,\ F = 23.87,\\
&p = 0.001,\ q^2 = 0.7491,\\
&\mathrm{DW} = 2.211 \quad \text{outliers}:\\
&\mathrm{A} = \mathrm{CH_2},\ \mathrm{B} = \mathrm{S},\ \mathrm{R_1} = \mathrm{H},\\
&\mathrm{R_2} = \mathrm{CF_3},\ \mathrm{Y} = \mathrm{NH_2};\quad \mathrm{A} = \mathrm{S},\\
&\mathrm{B} = \mathrm{CH_2},\ \mathrm{R_1} = 7\mathrm{F},\ \mathrm{R_2} = \mathrm{CN},\\
&\mathrm{Y} = \mathrm{NH_2} \qquad \text{(model 4)}
\end{aligned}$$

Model 4 is developed for COX-1 inhibitory activity data upon eliminating compounds 3 and 15 as outliers. The reason for the outlying behaviour of compound 15 is same as discussed under model 1. Compound 3 is the only compound with thiochromanone type fusion between central pyrazole ring and non-sulfonyl benzene ring among the congener. a_nS is a 2D molecular descriptor of MOE. It is the function of count of sulfur atoms of the ligand. The positive coefficient of a_nS indicates that isothiochromanone type fusion between central pyrazole core and non-sulfonyl benzene ring is conducive for COX-2 inhibitory activity. This finding is in good agreement with our preliminary observation of these compounds reported elsewhere.[12] In this preliminary Hansch type 2D QSAR analysis, we reported that the isothiochromanone ring type fusion as crucial for COX inhibitory activity of these compounds. In fact the contribution of a_nS supplements this earlier finding. Balaban *J* is one of the connectivity topological indices. Its contribution shows a negative effect on COX-1 inhibitory activity. The $|r|$ value of 0.370 between a_nS and Balaban *J* shows the absence of pair wise collinearity among them in model 4.

$$\begin{aligned}
&\log[IC_{50(\mathrm{COX\text{-}1})}/IC_{50(\mathrm{COX\text{-}2})}] = 58.047(\pm7.679)\\
&\mathrm{Balaban}\ J - 88.269(\pm11.890)\\
&n = 12,\ r = 0.923,\ r^2 = 0.851,\\
&r^2_{\mathrm{Adj}} = 0.836,\ s = 0.315,\ F = 57.14,\\
&p = 0.000,\ q^2 = 0.7989,\ \mathrm{DW} = 2.261 \qquad \text{(model 5)}
\end{aligned}$$

Model 5 is developed for selective COX-2 inhibition over COX-1 for the same 12 compounds used for COX-1 inhibitory activity modelling. The topological index Balaban *J* explains 83.6% variance in selective COX-2 inhibition over COX-1. It shows a positive effect towards selectivity among this congener.

$$\begin{aligned}
&\log[IC_{50(\mathrm{COX\text{-}1})}/IC_{50(\mathrm{COX\text{-}2})}]\\
&\quad = 5.530(\pm0.456)C^8 + 2.286(\pm0.091)\\
&n = 9,\ r = 0.977,\ r^2 = 0.955,\\
&r^2_{\mathrm{Adj}} = 0.948,\ s = 0.177,\ F = 147.28,\\
&p = 0.000,\ q^2 = 0.9327,\\
&\mathrm{DW} = 2.319 \quad \text{outliers}: \mathrm{A} = \mathrm{S},\ \mathrm{B} = \mathrm{CH_2},\\
&\mathrm{R_1} = 7\mathrm{OCH_3},\ \mathrm{R_2} = \mathrm{CF_3},\ \mathrm{Y} = \mathrm{NH_2};\\
&\mathrm{A} = \mathrm{S},\ \mathrm{B} = \mathrm{CH_2},\ \mathrm{R_1} = 8\mathrm{F},\ \mathrm{R_2} = \mathrm{CF_3},\\
&\mathrm{Y} = \mathrm{NH_2};\quad \mathrm{A} = \mathrm{S},\ \mathrm{B} = \mathrm{CH_2},\\
&\mathrm{R_1} = 7\mathrm{OCH_3},\ 8\mathrm{F},\ \mathrm{R_2} = \mathrm{CF_3},\ \mathrm{Y} = \mathrm{NH_2} \qquad \text{(model 6)}
\end{aligned}$$

Model 6 is developed for selective COX-2 over COX-1 inhibition, upon eliminating compounds 6, 10 and 7 as outliers. The contribution of C^8 in model 6 suggests that selectivity could be influenced by substitution at eighth position of the non-sulfonyl benzene ring.

In conclusion, the conformational flexibility of 1,5-diaryl pyrazoles with their central pyrazole ring fused to the non-sulfonyl benzene ring was examined using a simple connection table representation. Correlation analysis of conformationally dependent and independent descriptors along with Wang–Ford charges calculated on non-hydrogen common atoms of the compounds resulted in statistically significant QSAR models. The derived models provide significant measures not only to improve COX-2 inhibitory activity but also the selective COX-2 over COX-1 inhibition among these congeners.

Acknowledgements

Authors S.P. and E.M. thank the University Grants Commission (UGC), New Delhi for the financial support for this research and the Tata elxsi, India for providing the MOE software. Author S.P. wishes to thank Dr. S. Bharti, School of life sciences, Indore, India for his valuable support for this research.

References and notes

1. Botting, J. H. *Drugs Today* **1999**, *35*, 225.
2. Gans, K. R.; Galbraith, W. K.; Roman, R. J.; Haber, S. B.; Kerr, J. S.; Schmidt, W. K.; Smith, C.; Hewes, W. E.; AcKerman, N. R. *J. Pharmacol. Exp. Ther.* **1990**, *254*, 180.
3. Penning, T. D.; Talley, J. J.; Bertenshaw, S. R.; Carter, J. S.; Collins, P. W.; Doctor, S.; Graneto, M. J.; Lee, L. F.; Malecha, J. W.; Miyashiro, J. M.; Rogers, R. S.; Rogier, D. J.; Yu, S. S.; Anderson, G. D.; Burton, E. G.; Cogburn, J. N.; Gregory, S. A.; Koboldt, C. M.; Perkins, W. E.; Seibert, K.; Veenhuizen, A. W.; Zhang, Y. Y.; Isakson, P. C. *J. Med. Chem.* **1997**, *40*, 1347.
4. Prasit, P.; Wang, Z.; Brideau, C.; Chan, C. C.; Charleson, S.; Cromlish, W.; Ethier, D.; Evans, J. F.; Ford-Hutchinson, A. W.; Gauthier, J. Y.; Gordon, R.; Guay, J.; Gresser, M.; Kargman, S.; Kennedy, B.; Leblanc, Y.; Leger, S.; Mancini, J.; O'Neill, G. P.; Ouellet, M.; Percival, M. D.; Perrier, H.; Riendeau, D.; Rodger, I. W.; Tagari, P.; Therien, M.; Vickers, P.; Wong, E.; Xu, L.-J.; Young, R. N.; Zambani, R.; Boyce, S.; Rupniak, N.; Forest, M.; Visco, D.; Patrick, D. *Bioorg. Med. Chem. Lett.* **1999**, *9*, 1773.
5. Talley, J. J.; Brown, D. L.; Carter, J. S.; Graneto, M. J.; Koboldt, C. M.; Masferrer, J. L.; Perkins, W. E.; Rogers, R. S.; Shaffer, A. F.; Zhang, Y. Y.; Zweiefel, B. S.; Seibert, K. *J. Med. Chem.* **2000**, *43*, 775.
6. Talley, J. J.; Bertenshaw, S. R.; Brown, D. L.; Carter, J. S.; Graneto, M. J.; Kellogg, M. S.; Koboldt, C. M.; Yuan, J.; Zhang, Y. Y.; Seibert, K. *J. Med. Chem.* **2000**, *43*, 1661.
7. Prasanna, S.; Manivannan, E.; Chaturvedi, S. C. *Bioorg. Med. Chem. Lett.* **2005**, *15*, 313.
8. Prasanna, S.; Manivannan, E.; Chaturvedi, S. C. *Bioorg. Med. Chem. Lett.* **2004**, *14*, 4005.
9. Prasanna, S.; Manivannan, E.; Chaturvedi, S. C. *QSAR Comb. Sci.* **2004**, *23*, 621.
10. Prasanna, S.; Manivannan, E.; Chaturvedi, S. C. *Indian J. Chem.* **2004**, *43B*, 2249.
11. Manivannan, E.; Prasanna, S.; Chaturvedi, S. C. *Indian J. Biochem. Biophys.* **2004**, *41*, 184.
12. Prasanna, S.; Manivannan, E.; Chaturvedi, S. C. *Arch. Pharm. Pharm. Med. Chem.* **2004**, *337*, 440.
13. Bertenshaw, S. R.; Talley, J. J.; Rogier, D. J.; Graneto, M. J.; Koboldt, C. M.; Zhang, Y.; Searle, G. D. *Bioorg. Med. Chem. Lett.* **1996**, *6*, 2827.
14. Durbin, J.; Watson, G. S. *Biometrika* **1951**, *38*, 159.
15. Roy, K.; Leonard, J. T.; Sengupta, C. *Bioorg. Med. Chem. Lett.* **2004**, *14*, 3705.
16. De, K.; Sengupta, C.; Roy, K. *Bioorg. Med. Chem.* **2004**, *12*, 3323.
17. Leonard, J. T.; Roy, K. *QSAR Comb. Sci.* **2004**, *23*, 387.
18. Dewar, M. J. S.; Zoebisch, E. G.; Healey, E. F.; Stewart, J. J. P. *J. Am. Chem. Soc.* **1985**, *107*, 3902.
19. Dewar, M. J. S.; Hwang, J. C.; Kuhn, D. R. *J. Am. Chem. Soc.* **1991**, *113*, 735.
20. Chem3D ultra version 6.0.1 is the software supplied by Cambridgesoft Corporation, USA.